

# Endogenous activation of metabotropic glutamate receptors in neocortical development causes neuronal calcium oscillations

Alexander C. Flint\*, Ryan S. Dammerman\*, and Arnold R. Kriegstein\*<sup>†‡</sup>

\*Center for Neurobiology and Behavior and <sup>†</sup>Department of Neurology, Columbia University, College of Physicians and Surgeons, New York, NY 10032

Edited by Dominick P. Purpura, Albert Einstein College of Medicine, Bronx, NY, and approved August 11, 1999 (received for review June 3, 1999)

Oscillations in intracellular free calcium concentration ( $[Ca^{2+}]_i$ ) occur spontaneously in immature neurons of the developing cerebral cortex. Here, we show that developing murine cortical neurons exhibit calcium oscillations in response to direct activation of the mGluR5 subtype of the group I metabotropic glutamate receptor (mGluR). In contrast, other manipulations that elicit  $[Ca^{2+}]_i$  increases produce simple, nonoscillatory changes. Furthermore, we find that spontaneous oscillatory  $[Ca^{2+}]_i$  activity is blocked by antagonists of group I mGluRs, suggesting a specific role for mGluR activation in the promotion of oscillatory  $[Ca^{2+}]_i$  dynamics in immature cortical neurons. The oscillatory pattern of  $[Ca^{2+}]_i$  increases produced by mGluR activation might play a role in the regulation of gene expression and the control of developmental events.

neuronal development | cortex

Spontaneous changes in the concentration of neuronal free calcium ( $[Ca^{2+}]_i$ ) have been observed in a variety of developing systems, many of which exhibit distinct spatial and temporal patterns of  $[Ca^{2+}]_i$  fluctuation (1–7). In the developing neocortex, several patterns of calcium dynamics have been described. Proliferative neuroepithelial cells in the embryonic ventricular zone display several patterns of  $[Ca^{2+}]_i$  dynamics, including isolated transients, coordinated  $[Ca^{2+}]_i$  increases in local cell clusters, and synchronous transients in cell pairs undergoing mitotic division (8). In the postnatal neocortex, coordinated  $[Ca^{2+}]_i$  rises can occur in 3–100 adjacent neurons, termed neuronal domains (9). These spontaneous events are mediated by gap junctional communication (10) and appear to involve cell-to-cell diffusion of the second messenger inositol trisphosphate (9, 11). Neocortical domains apparently can occur independently of action potential activity, but their frequency can be increased by activation of metabotropic glutamate receptors (mGluR) (11). Activation of ionotropic glutamate and  $\gamma$ -aminobutyric acid (GABA) receptors can cause elevations in  $[Ca^{2+}]_i$  in developing neocortical neurons, and synaptic activation of these neurons can lead to monophasic  $[Ca^{2+}]_i$  transients (12, 13). Application of mGluR agonists has been observed to produce oscillations in  $[Ca^{2+}]_i$  in neurons and glia in the developing hippocampus and neocortex (14, 15). Spontaneous oscillatory changes in  $[Ca^{2+}]_i$  have also been observed in single developing neocortical neurons (8, 12, 16), but their mode of activation has not been characterized.

Of the various patterns of  $[Ca^{2+}]_i$  dynamics, oscillations in  $[Ca^{2+}]_i$  during development may be of particular importance in signal transduction and the regulation of gene expression (17, 18). In some systems  $[Ca^{2+}]_i$  oscillations of different frequency can be transduced into specific intracellular signals (19, 20). Recent work has also shown that the frequency and duration of  $[Ca^{2+}]_i$  oscillations can differentially influence the expression of specific genes (21–23). One known mechanism for the generation of  $[Ca^{2+}]_i$  oscillations by cell-to-cell signaling involves activation of the mGluR5 subtype of the group I mGluRs, which are highly expressed in the immature neocortex (16, 24, 25).

Activation of mGluR5 leads to the production of inositol trisphosphate by phospholipase C, which, in turn, leads to increases in  $[Ca^{2+}]_i$ . Little is known, however, about the role that mGluR signaling plays in the physiology of developing neocortical neurons.

To investigate the potential role of mGluR activation in generating spontaneous  $[Ca^{2+}]_i$  oscillations in developing neocortical neurons, we performed a series of calcium imaging experiments using embryonic and postnatal mouse neocortical slices. We found that activation of the mGluR5 subtype of mGluRs leads to  $[Ca^{2+}]_i$  oscillations in immature neurons, and that endogenous glutamate acting on group I mGluRs is responsible for spontaneous  $[Ca^{2+}]_i$  oscillations in developing neocortex.

## Methods

**Tissue Preparation.** Coronal slices of neocortex (300–400  $\mu$ m) were prepared from neonatal or embryonic Swiss–Webster mice (Taconic Farms) by using a Vibratome (Pelco, Redding, CA) as previously described (13). For embryonic slices, brains were embedded in 4% low-melting agarose (Fisher Scientific) in PBS with glucose (Life Technologies, Grand Island, NY) prior to slicing. Slices were prepared and incubated in standard artificial cerebrospinal fluid (ACSF), which contains 125 mM NaCl, 2.5 mM KCl, 1.25 mM  $NaH_2PO_4$ , 1 mM  $MgSO_4$ , 2 mM  $CaCl_2$ , 25 mM  $NaHCO_3$ , and 20 mM glucose (pH 7.4), oxygenated with 95%  $O_2$ /5%  $CO_2$ . Following slice preparation, slices were incubated in ACSF at room temperature for 15 min prior to loading with the indicator dye.

**Fluo-3 Loading.** Cells were loaded with the calcium indicator dye fluo-3 by bath application of fluo-3 acetoxymethyl ester (fluo-3-AM; Molecular Probes). Loading was performed for 1–4 hr at room temperature in ACSF containing 15  $\mu$ M fluo-3-AM, 0.0067% pluronic F-127 (Molecular Probes), and 0.33% DMSO (Sigma). The loading chamber was continuously oxygenated with 95%  $O_2$ /5%  $CO_2$ .

**Calcium Imaging.** Measurements of relative changes in  $[Ca^{2+}]_i$  were made using vital epifluorescence microscopy of mouse neocortical slices loaded with fluo-3. For imaging, slices were removed from the loading solution to standard oxygenated

This paper was submitted directly (Track II) to the PNAS office.

Abbreviations: mGluR, metabotropic glutamate receptor; ACSF, artificial cerebrospinal fluid; NMDA, *N*-methyl-D-aspartate; ACh, acetylcholine; *trans*-ACPD, 1-aminocyclopentane-*trans*-1,3-dicarboxylic acid; HPG, hydroxyphenylglycine; DHPG, dihydroxyphenylglycine; CPG, carboxyphenylglycine; TTX, tetrodotoxin; DNQX, 6,7-dinitroquinoxaline-2,3-dione; 5-HT, serotonin; *D*-AP5, *D*(-)-2-amino-5-phosphonopentanoic acid; DCG-IV, (2*S*,2'*R*,3'*R*)-2-(2',3'-dicarboxycyclopropyl)glycine; *L*-AP4, (+)-2-amino-4-phosphonobutyric acid; *Pn*, postnatal day *n*.

<sup>‡</sup>To whom reprint requests should be addressed. E-mail: ark17@columbia.edu.

The publication costs of this article were defrayed in part by page charge payment. This article must therefore be hereby marked "advertisement" in accordance with 18 U.S.C. §1734 solely to indicate this fact.

ACSF, transferred to a recording chamber on the stage of an upright compound microscope (Olympus BX50-WI, Tokyo, Japan), and perfused with oxygenated ACSF at a rate of 1–2 ml/min. Epifluorescence imaging of fluo-3 intensity was performed with a 100-W mercury light source and a low-light charge-coupled device video camera (Dage-MTI 300-T, Michigan City, IN). Fluorescence filters (Chroma Technology, Brattleboro, VT) for fluo-3 imaging were as follows: excitation filter,  $480 \pm 20$  nm; dichroic mirror, 505 nm longpass; and emission filter,  $535 \pm 25$  nm. Images were acquired using a  $10\times$  water-immersion objective. Time-lapse sequences of fluo-3 fluorescence were acquired using custom macros within the public domain National Institutes of Health IMAGE program (available on the Internet at <http://rsb.info.nih.gov/nih-image/>) on a Macintosh computer equipped with a video frame acquisition board (Scion Corporation, Frederick, MD). Minimal exposure of the preparation to the excitation light was achieved by controlling a shutter in the excitation light path (Uniblitz vs.25; Vincent Associates, Rochester, NY) through digital outputs of the frame acquisition board. Video-rate acquisition of frames minimized exposure ( $<500$  ms) of the tissue at each timed shutter opening. Each frame in a time-lapse sequence was captured every 3–4 s. Gain, black level, and number of accumulated video frames per final frame were empirically adjusted to minimize background and maximize peak response intensity without causing saturation at either end of the signal. If saturation of responses was observed, the data were discarded and the experiment was repeated at nonsaturating gain levels. Slice viability was monitored by visualization of cellular integrity under infrared differential interference contrast videomicroscopy and/or by visualizing calcium responses to *N*-methyl-D-aspartate (NMDA;  $50 \mu\text{M}$ ) or acetylcholine (ACh;  $100 \mu\text{M}$ ).

**Drug Application.** Pharmacological agents were applied by a multi-valve, single-output focal drug application device (ALA Scientific, Westbury, NY). Several (five to eight) frames of baseline were recorded during focal application of control ACSF, and then drug-containing ACSF was applied for the remainder of the imaging series. Following an imaging series, control ACSF was again focally applied to wash out the applicator tip and to facilitate washout of the drug from the slice. A minimum intertrial time of 10 min in the presence of flowing bath and focally applied control ACSF was used in all experiments. Stock drug solutions were prepared at the indicated concentrations in equimolar NaOH: 10 mM 1-aminocyclopentane-*trans*-1,3-dicarboxylic acid (*trans*-ACPD)/10 mM quisqualate/100 mM (*R,S*)-3,5-dihydroxyphenylglycine (DHPG)/100 mM *S*-3-hydroxyphenylglycine (HPG)/100 mM *S*-4-carboxyphenylglycine (CPG). The following drug stocks were prepared in the indicated solvents: (*2S,2'R,3'R*)-2-(2',3'-dicarboxycyclopropyl)glycine (DCG-IV; 10 mM in  $\text{H}_2\text{O}$ ), L(+)-2-amino-4-phosphonobutyric acid (L-AP4; 10 mM in  $\text{H}_2\text{O}$ )/NMDA (10 mM in  $\text{H}_2\text{O}$ ), tetrodotoxin (TTX; 3 mM in  $\text{H}_2\text{O}$ ), 6,7-dinitroquinoxaline-2,3-dione (DNQX; 100 mM in DMSO), ACh (10 mM in  $\text{H}_2\text{O}$ ), serotonin (5-HT; 10 mM in  $\text{H}_2\text{O}$ ), and D(-)-2-amino-5-phosphonopentanoic acid (D-AP5; 10 mM in  $\text{H}_2\text{O}$ ). The above stock solutions were aliquoted for single use and stored at  $-20^\circ\text{C}$ . For the mGluR selective agents, stocks were only used for 1 wk (ACPD; *R,S*-3, 5-DHPG; *S*-4-CPG; DCG-IV; L-AP4) or 1 day (*S*-3-HPG) before fresh stocks were prepared. Caffeine was prepared fresh in ACSF at 10 mM. All drugs were obtained from Research Biochemicals (Natick, MA), Tocris Cookson (Ballwin, MO), or Sigma.

**Analysis of Calcium Imaging.** Quantification of relative changes in  $[\text{Ca}^{2+}]_i$  was performed by measuring changes in fluo-3 fluorescence as a function of time using National Institutes of Health IMAGE software on a Macintosh computer. Areas over indi-

vidual cells were selected, and the mean intensity at each frame was measured. Raw data were in the form of a linear 0–255 arbitrary units intensity scale. Raw data were then exported to Microsoft Excel software for conversion to a percentage relative change in fluorescence over background fluorescence ( $\% \Delta F/F$ ) scale for comparison across experiments (26, 27). In some situations, moderate bleaching of the fluorescence signal across all cells in the slice was observed, but the extent of bleaching was always  $<10\%$  of the background fluorescence, and the progression of bleaching was always linear as a function of time when averaged across the slice. In cases where bleaching was observed, it was corrected for post hoc by adding a linear adjustment factor determined by measurement of the bleaching rate over inactive regions. Final  $\% \Delta F/F$  data were exported to DeltaGraph software for statistical analysis and graphing. For event analysis of active neurons and quantification of interevent intervals of calcium oscillations, events were defined as changes in fluorescence that exceeded 25%  $\Delta F/F$  and returned to levels below this threshold. Cellular responses displaying three or more events during the imaging time window were considered oscillatory.

**Biocytin Labeling of Neurons and Glia.** To demonstrate the distinct morphologies of immature neocortical neurons and glia, patch-clamp recordings were made from neocortical slices as previously described (28). Recording pipettes were filled with a solution of 140 mM KCl/5 mM EGTA/3 mM  $\text{MgCl}_2$ /5 mM HEPES/1% (wt/vol) biocytin (pH 7.3) at room temperature. Following recording to confirm neural or glial electrophysiologic characteristics and to allow for intracellular biocytin diffusion, slices were fixed in 4% paraformaldehyde in PBS overnight, washed in PBS, resectioned at  $75 \mu\text{m}$ , and processed for biocytin avidin/peroxidase histochemistry (Vector Laboratories). Images of filled cells were acquired on a Zeiss Axioskop microscope with a  $40\times$  objective and a Kodak DC120 digital camera.

## Results

**mGluR Activation Causes Calcium Oscillations in the Developing Neocortex.** The metabotropic glutamate receptor agonist *trans*-ACPD ( $40 \mu\text{M}$ ) was focally applied to fluo-3-loaded slices of somatosensory cortex prepared from first week postnatal mice. Cells that responded to *trans*-ACPD exhibited either a single peak in relative  $[\text{Ca}^{2+}]_i$  with return to baseline levels ( $11 \pm 6\%$ , mean  $\pm$  SD), a sustained increase in  $[\text{Ca}^{2+}]_i$  ( $14 \pm 5\%$ ), or oscillatory changes in relative  $[\text{Ca}^{2+}]_i$  ( $74 \pm 6\%$ , Fig. 1A,  $n = 3$  slices). Responding cells were of typical pyramidal neuronal morphology based on their fluo-3 fluorescence (Figs. 1A and 3A) as well as their appearance when examined under higher power with infrared differential interference contrast videomicroscopy. During *trans*-ACPD applications, we also observed an increased frequency of coordinated “domains” of calcium elevation in adjacent cells, as has been previously reported (11). Whereas the oscillatory responses occurred within seconds of *trans*-ACPD application, the increased frequency of calcium domains was usually associated with long-term ( $>20$  min) application of *trans*-ACPD. Because drug-evoked oscillatory calcium dynamics confined to single cells have not been well characterized for developing neocortical neurons, and because metabotropic receptors have been implicated in the control of oscillatory calcium dynamics (24, 25), we focused our analysis on single or individual cells that oscillated in response to *trans*-ACPD. Fig. 1A shows the fluo-3 fluorescence of one such cell during its oscillatory response to *trans*-ACPD, and its relative percent change in fluorescence ( $\% \Delta F/F$ ).

The frequency of  $[\text{Ca}^{2+}]_i$  oscillations evoked by *trans*-ACPD varied across cells, with a range of 8–80 s between peaks of  $[\text{Ca}^{2+}]_i$  in the sustained presence of *trans*-ACPD ( $n = 30$  slices). Analysis of the distribution of interpeak intervals showed that

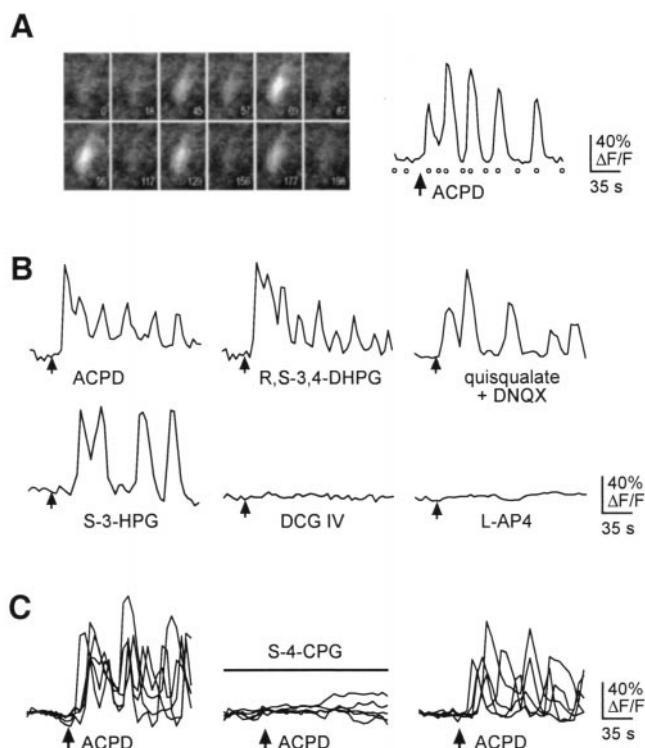


**Fig. 1.** Activation of intracellular calcium ( $[Ca^{2+}]_i$ ) oscillations by group I mGluRs in developing neocortex. (A) Example of an oscillatory intracellular free calcium response caused by the mGluR agonist *trans*-ACPD ( $40 \mu M$ ). (Left) The fluorescence of a single fluo-3-loaded neuron at several times during imaging. The elapsed time is shown in the lower right corner of each frame. (Right) This cell's response, measured as  $\% \Delta F/F$ . Open circles indicate the times of the corresponding frames shown at left. ACPD application began at the arrow and continued until the end of the imaging series. (B) The group I mGluR agonists *R,S*-3,4-DHPG ( $100 \mu M$ ), quisqualate ( $10 \mu M$ ) in the presence of DNQX ( $10 \mu M$ ), and *S*-3-HPG ( $300 \mu M$ ) all produced oscillatory  $[Ca^{2+}]_i$  responses, whereas agonists of group II mGluRs (DCG-IV,  $1 \mu M$ ) and group III mGluRs (*L*-AP4,  $100 \mu M$ ) did not produce  $[Ca^{2+}]_i$  oscillations in these cells. (C) Oscillatory  $[Ca^{2+}]_i$  changes induced by *trans*-ACPD were reversibly abolished by the specific group I mGluR antagonist *S*-4-CPG ( $1 mM$ ). Five oscillatory responses to *trans*-ACPD are shown in the Left, and the block of this response and subsequent recovery in the same neurons are shown in the following traces.

the mean period was  $28 \pm 18$  s and the modal period was 16 s. The frequency of oscillations did not change significantly as a function of age within the first postnatal week (mean period at P0/1,  $27 \pm 16$  s, mean period at P6/7,  $28 \pm 18$ ,  $P = 0.47$ , Student's *t* test). Excluding the first peak of the response to the initial application of *trans*-ACPD, oscillations occurring in different cells were not temporally correlated in any obvious manner (see Figs. 1C and 3B).

**Group I mGluRs Are Responsible for Calcium Oscillation in the Developing Neocortex.** To determine the type of mGluR responsible for the production of calcium oscillations, we performed experiments with agonists and antagonists of specific mGluRs. Calcium oscillations could be elicited by several agonists with reported selectivity for group I mGluRs. Application of the group I-specific agonists *RS*-3,4-DHPG ( $500 \mu M$ ,  $n = 3$  slices) or *S*-3-HPG ( $300 \mu M$ ,  $n = 4$  slices) produced oscillatory calcium responses, mimicking the action of *trans*-ACPD ( $40 \mu M$ ) (Fig. 1B). Similarly, application of quisqualate ( $10 \mu M$ ), which has selectivity for group I receptors, along with DNQX ( $10 \mu M$ ) to block the effects of quisqualate on non-NMDA ionotropic

glutamate receptors, also caused  $[Ca^{2+}]_i$  oscillations (Fig. 1B,  $n = 4$  slices). These three manipulations to activate group I mGluRs produced a range of oscillatory and simple responses that were qualitatively indistinguishable from those induced by *trans*-ACPD.

In contrast, application of DCG-IV ( $1 \mu M$ ), a specific agonist of group II mGluRs, had no discernable effect on  $[Ca^{2+}]_i$  (Fig. 1B,  $n = 4$  slices). Likewise, application of the selective group III mGluR agonist *L*-AP4 ( $100 \mu M$ ) did not cause changes in  $[Ca^{2+}]_i$  (Fig. 1B,  $n = 3$  slices). Therefore, it appears that, in the developing neocortex, group I mGluRs are responsible for mGluR-mediated calcium responses in general and calcium oscillations in particular. To confirm this observation, we performed experiments with a selective antagonist of group I mGluRs, *S*-4-CPG ( $1 mM$ ). *S*-4-CPG reversibly blocked the oscillatory responses to *trans*-ACPD as shown in Fig. 1C ( $n = 3$  slices). Therefore, we conclude that group I mGluRs are the subclass of mGluR responsible for the production of calcium oscillations in developing neocortex.

**mGluR5 Is the Specific mGluR Isoform That Causes Neocortical Calcium Oscillations.** Experiments with expression systems and cultured astrocytes have shown specific roles for the two group I mGluRs (mGluR1 and mGluR5) in the control of intracellular calcium dynamics. Activation of mGluR1 has been shown to cause sustained elevations in  $[Ca^{2+}]_i$ , whereas mGluR5 activation can also cause oscillations in  $[Ca^{2+}]_i$  (24, 25). Of the two group I mGluRs, only mGluR5 is expressed in the first week postnatal neocortex (29), thereby implicating this isoform in the oscillations we have observed. Expression of both mGluR5 protein and mRNA is abundant in rat cortex at P1 (29), suggesting that expression begins *in utero*. Indeed, application of *trans*-ACPD to slices of E19 neocortex produced oscillatory responses as shown in Fig. 2A ( $n = 3$  slices). To support a specific role of mGluR5 in generating oscillations, we performed calcium imaging experiments on another neuronal population that expresses mGluR5, but not mGluR1, and a population that expresses mGluR1, but not mGluR5. Early postnatal hippocampal pyramidal cells express mGluR5 and respond to *trans*-ACPD with calcium oscillations (Fig. 2B,  $n = 4$  slices). In agreement with previous studies (30), mGluR1-expressing cerebellar Purkinje cells at P14 responded to *trans*-ACPD with simple, nonoscillatory responses (Fig. 2C,  $n = 3$  slices). These data confirm that mGluR5 is indeed the specific isoform of mGluR responsible for causing calcium oscillations in neocortical neurons.

**Calcium Oscillations in the Early Developing Cortex Occur as a Result of Direct Activation of mGluRs on Neurons.** Previous studies have shown that neocortical glial cells in culture and hippocampal glial cells in slices can produce  $[Ca^{2+}]_i$  oscillations (31–33). Therefore, we examined whether neurons respond directly to mGluR activation with  $[Ca^{2+}]_i$  oscillations. There are very few astrocytes present in neocortex in the embryonic and early postnatal periods when mGluR oscillations are observed. Neurons and glia can be distinguished in postnatal fluo-3-loaded slices on the basis of their morphology. Fig. 3A shows a P3 pyramidal neuron and a P15 glial cell, both filled with the intracellular tracer biocytin to highlight the obvious morphological differences between these cells. The same morphological differences in size and cell body shape can be discerned in the fluorescence images of fluo-3-loaded neurons and glia, as shown in the *Insets* in Fig. 3A. This distinction can also be made by visualization of cells under infrared differential interference contrast videomicroscopy. Therefore, we were able to focus on responses to mGluR activation selectively in cells with neuronal morphology.

We performed additional experiments to confirm the activation of mGluRs on neurons. Slices were first exposed to a



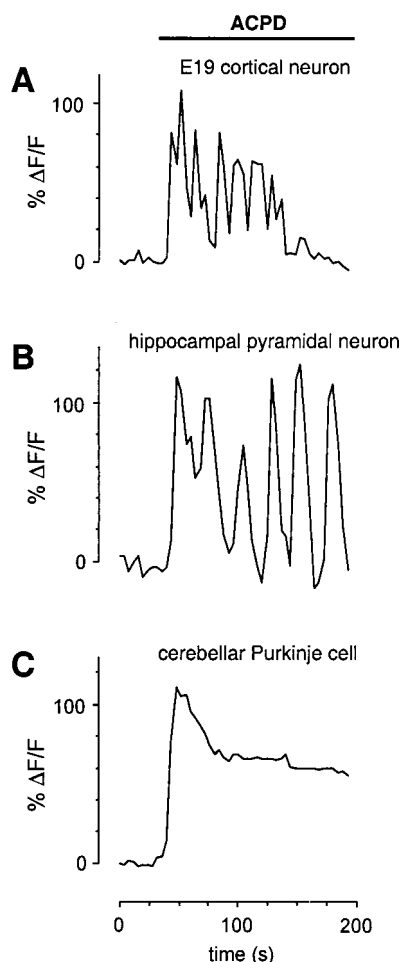


**Fig. 2.** Oscillatory responses are only observed in cells expressing mGluR5. (A) Oscillatory responses to *trans*-ACPD were observed at embryonic day 19 (E19), when mGluR5 is first expressed in the developing neocortex. (B) Oscillatory *trans*-ACPD responses were also observed in the postnatal hippocampus (P6) where mGluR5 is also expressed. (C) Simple, nonoscillatory  $[Ca^{2+}]_i$  responses to *trans*-ACPD were observed in cerebellar Purkinje cells at P14. These neurons express mGluR1 but do not express mGluR5.

combination of TTX (1  $\mu$ M), DNQX (10  $\mu$ M), and D-AP5 (100  $\mu$ M) to block action potentials and ionotropic glutamate receptor activation. In the presence of these blockers, *trans*-ACPD (40  $\mu$ M) was applied, producing oscillations like those seen in the absence of the blockers (Fig. 3B,  $n = 12$  slices). Similar experiments performed with kynurenic acid (1 mM), a nonselective ionotropic glutamate receptor antagonist, yielded the same results (data not shown;  $n = 10$  slices). These data suggest that *trans*-ACPD acts directly on the responding cells, but we cannot exclude the possibility that glial cells release a nonsynaptic signal that is insensitive to blockers of fast synaptic transmission and ionotropic glutamate receptors. To prove the neuronal identity of responding cells, D-AP5 was removed from the combination of blockers to allow for NMDA receptor activation, and then NMDA (30  $\mu$ M) was applied to the slice. Because neocortical glial cells do not express NMDA receptors, they do not respond to NMDA with calcium increases (34). Therefore, the direct response to NMDA of the cells that oscillated in response to *trans*-ACPD demonstrates that they are neurons (Fig. 3B;  $n = 6$  slices).

**Oscillatory Calcium Responses Are Not an Intrinsic Property of Intracellular Calcium Release in Immature Cortical Neurons.** To determine whether calcium oscillations are specific to mGluR

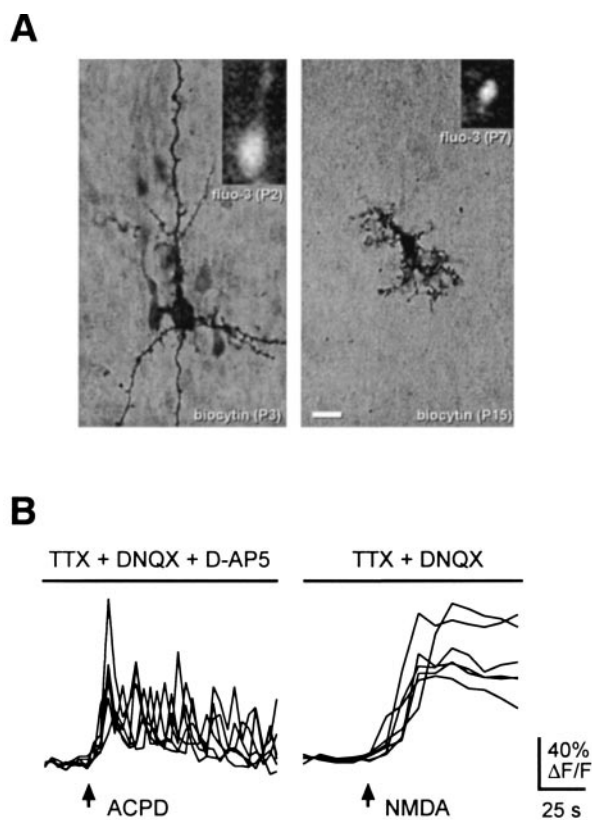


**Fig. 3.**  $[Ca^{2+}]_i$  oscillations occur by direct activation of mGluRs on neurons. (A) Neurons and glia can be readily distinguished in fluo-3-loaded slices. A biocytin-filled neuron in a P3 neocortical slice shown in comparison to a biocytin-filled glial cell from an older slice (P15) highlights the difference in size and morphological features between these cell types (main panels). The size difference can be appreciated on visualization of fluo-3-loaded neurons and glia (insets). (B) Cells with neuronal morphology exhibit oscillatory  $[Ca^{2+}]_i$  dynamics on direct activation of mGluRs when indirect stimulation of these cells is blocked with TTX (1  $\mu$ M), DNQX (10  $\mu$ M), and D-AP5 (100  $\mu$ M). Given the exclusive expression of NMDA receptors by neurons in the neocortex, we subsequently confirmed neuronal identity by observing direct calcium responses of these same cells to NMDA (30  $\mu$ M) in the presence of TTX (1  $\mu$ M) and DNQX (10  $\mu$ M).

activation in immature cortical neurons, we used agonists known to activate other metabotropic receptor types expressed in the developing cortex. Application of ACh (100  $\mu$ M) to P1 slices caused a significant rise in  $[Ca^{2+}]_i$  in nearly every fluo-3-loaded cell (Fig. 4A;  $n = 4$  slices). The response in all cases was a simple, sustained response without oscillatory fluctuation. Similarly, most cells in P1 slices responded to the application of 5-HT (100  $\mu$ M) with simple responses that decremented slightly over time, and in no case were oscillations observed in response to 5-HT (Fig. 4B,  $n = 5$  slices). Responses to ACh and 5-HT were not blocked by TTX (1  $\mu$ M;  $n = 3$  slices each condition), indicating that the cells responded directly to these transmitters.

We also tested the response of neurons to caffeine (10 mM), which causes release of calcium from internal stores by activation of the ryanodine receptor. We found that many cells in slices at both P0/1 and P6/7 responded to caffeine with simple rises in  $[Ca^{2+}]_i$ , and no cells displayed oscillations in  $[Ca^{2+}]_i$  (Fig. 4C;  $n = 7$  slices). These results demonstrate that intracellular calcium release in immature cortical neurons is not intrinsically oscillatory, but that oscillations are specific to mGluR5 activation.

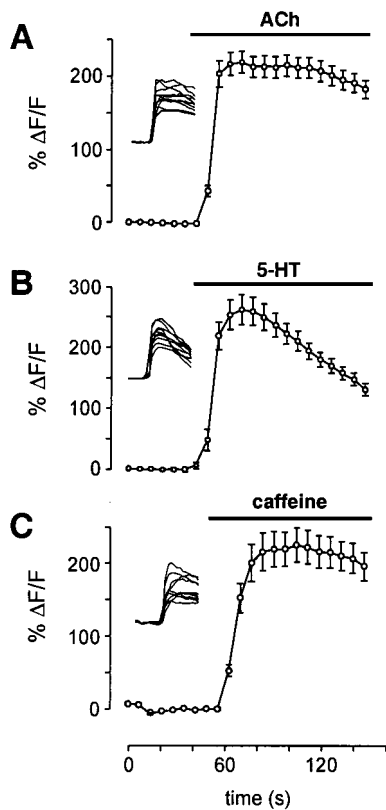


**Fig. 4.** Other signaling systems that activate calcium release from internal stores do not cause calcium oscillations. (A) Simple, nonoscillatory rises in  $[Ca^{2+}]_i$  were observed in response to ACh (100  $\mu$ M). Data are plotted as mean  $\pm$  SEM, and the raw data from individual cells are shown in the *Inset*. (B) 5-HT (100  $\mu$ M) also produced simple calcium responses. (C) Similar nonoscillatory responses occurred on application of caffeine (10 mM), which causes calcium release activated by ryanodine receptors.

**Endogenous Glutamate Acting on mGluRs Produces Spontaneous Calcium Oscillations in Developing Cortex.** Calcium imaging of neocortical slices in control ACSF reveals several patterns of spontaneous  $[Ca^{2+}]_i$  fluctuation (8, 9, 12, 13, 35). Some of this activity can be eliminated by manipulations that block fast synaptic transmission or action potentials (12, 13). Many cells, however, continue to display spontaneous calcium transients under these conditions, and much of this remaining activity is oscillatory. To address whether mGluRs might have a role in these endogenous oscillatory events, we examined the effects of the specific group I mGluR antagonist *S*-4-CPG on calcium activity persisting in the presence of TTX (1  $\mu$ M), DNQX (10  $\mu$ M), and D-AP5 (100  $\mu$ M) (Fig. 5). We found that this combination of blockers of action potentials and ionotropic glutamatergic synaptic transmission reduced the number of cells displaying spontaneous changes in  $[Ca^{2+}]_i$  to  $38.4 \pm 5.4\%$  of control ( $n = 6$  slices). We then added the group I mGluR blocker *S*-4-CPG (1 mM). Remarkably, the addition of *S*-4-CPG almost entirely blocked the ongoing spontaneous calcium activity observed in TTX, DNQX, and D-AP5 (Fig. 5 *A* and *B*;  $n = 7$  slices,  $P \ll 0.001$ , Student's *t* test). *S*-4-CPG reduced the number of cells displaying calcium transients to 6.6% of the number observed in the mixture of blockers. Almost all of the residual activity observed in the presence of TTX, DNQX, D-AP5, and *S*-4-CPG consisted of relatively slow changes in  $[Ca^{2+}]_i$ , and none of the cells observed under these conditions displayed oscillatory dynamics of the type elicited by mGluR activation. Therefore, these data demonstrate that endogenous glutamate

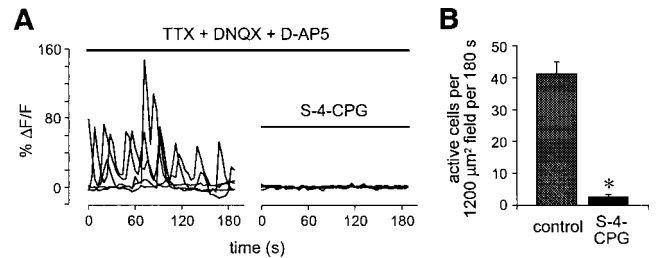


**Fig. 5.** Endogenous glutamate acting on mGluRs significantly contributes to spontaneous calcium dynamics in the developing neocortex. (A) A subset of neurons exhibiting spontaneous, oscillatory calcium dynamics (approximately 40%) continues to display these calcium dynamics in the presence of TTX (1  $\mu$ M), DNQX (10  $\mu$ M), and D-AP5 (100  $\mu$ M). Subsequent coapplication of the group I-specific mGluR antagonist *S*-4-CPG blocks this remaining spontaneous oscillatory activity. (B) The near abolition of spontaneous  $[Ca^{2+}]_i$  transients in the presence of *S*-4-CPG is quantified ( $n = 7$  slices, >200 active cells before *S*-4-CPG; \*,  $P \ll 0.001$ , Student's *t* test).

acts on group I mGluRs in neonatal cortical slices to generate oscillations in  $[Ca^{2+}]_i$ . In addition, because the spontaneous activity that was blocked by *S*-4-CPG persisted in the presence of TTX, it appears that the source of endogenous glutamate is not dependent on action potential-mediated release.

## Discussion

In astrocytes and expression systems, activation of the mGluR5 subtype of group I mGluRs has been shown to induce oscillatory changes in  $[Ca^{2+}]_i$  (25). This oscillatory response is in contrast to the simple  $[Ca^{2+}]_i$  transient evoked by activation of the other, identified group I mGluR isoform, mGluR1. The structural difference between the two isoforms that produces this functional difference has been identified as a phosphorylation site present in mGluR5 but absent in mGluR1 (24). A mechanism by which mGluR5 activation leads to calcium oscillations has recently been proposed (24). On activation of mGluR5, both diacylglycerol (DAG) and inositol trisphosphate are produced. Inositol trisphosphate production leads to an increase in intracellular free  $[Ca^{2+}]_i$ , whereas DAG activates protein kinase C (PKC), which in turn phosphorylates mGluR5, thus inhibiting it. This inhibition allows calcium levels to fall and the production of DAG to end, thereby decreasing the activation of PKC and the phosphorylation of mGluR5. With dephosphorylation of mGluR5 the cycle begins again, and the  $[Ca^{2+}]_i$  oscillations will occur in the continued presence of the extracellular ligand.

The oscillatory nature of the mGluR5-mediated response is distinct from the simple nonoscillatory transients observed in cortical neurons or neuroblasts on activation of ionotropic glutamate or  $\gamma$ -aminobutyric acid (GABA) receptors, or on application of other neurotransmitters (8, 12, 27). Of the various patterns of  $[Ca^{2+}]_i$  dynamics, oscillations in  $[Ca^{2+}]_i$  during development may be of particular importance in signal transduction and the regulation of gene expression (17, 18). Oscillations of  $[Ca^{2+}]_i$  of varying frequency can be transduced into specific intracellular signals by enzymes such as calcium-sensitive mitochondrial dehydrogenases (36) and calcium/calmodulin-dependent protein kinase II (CAMKII) (19, 20), an enzyme believed to be involved in certain forms of synaptic plasticity (37–39). Experiments in several cell types have shown that the frequency of  $[Ca^{2+}]_i$  oscillations can also influence the expression of specific genes (21, 23), and that calcium oscillations of varying frequency can produce different patterns of gene expression in the same cell type (22). In rodent neocortex, mGluR5 expression is highest during the first two postnatal weeks (29). This is an ontological period characterized by peak levels of synaptogenesis and synaptic plasticity (40–42). Because  $[Ca^{2+}]_i$

oscillations can be involved in signal transduction events and in the regulation of gene expression, mGluR5-induced  $[Ca^{2+}]_i$  oscillations are a potential mechanism for epigenetic control of gene expression during a critical period of cortical development.

In summary, we have found that activation of the group I mGluR, mGluR5, on developing neocortical neurons leads to oscillations in  $[Ca^{2+}]_i$ . These oscillations are not a general feature of metabotropic receptor activation, but rather they are the result of a specific signaling system downstream of mGluR5. Oscillations mediated by mGluRs are found to contribute significantly to spontaneous calcium dynamics in the immature

cortex, such that nearly all spontaneous calcium transients can be accounted for by a combination of fast synaptic signaling and glutamate acting on mGluRs. As specific types of calcium dynamics have been shown to be critical in the regulation of gene expression (21, 43, 44) and the control of developmental events (22, 45, 46), this newly discovered role for mGluRs in the neocortex is likely to influence early neuronal maturation.

We thank David Owens for helpful suggestions. This work was supported by Grants NS 21223 and NS 35710 from the National Institutes of Health, and a grant from the March of Dimes Birth Defects Foundation.

1. Gu, X., Olson, E. C. & Spitzer, N. C. (1994) *J. Neurosci.* **14**, 6325–6335.
2. Spitzer, N. C., Olson, E. & Gu, X. (1995) *J. Neurobiol.* **26**, 316–324.
3. Spitzer, N. C. (1994) *Trends Neurosci.* **17**, 115–118.
4. Wong, R. O., Meister, M. & Shatz, C. J. (1993) *Neuron* **11**, 923–938.
5. Wong, R. O., Chernjavsky, A., Smith, S. J. & Shatz, C. J. (1995) *Nature (London)* **374**, 716–718.
6. Penn, A. A., Riquelme, P. A., Feller, M. B. & Shatz, C. J. (1998) *Science* **279**, 2108–2112.
7. Katz, L. C. & Shatz, C. J. (1996) *Science* **274**, 1133–1138.
8. Owens, D. F. & Kriegstein, A. R. (1998) *J. Neurosci.* **18**, 5374–5388.
9. Yuste, R., Peinado, A. & Katz, L. C. (1992) *Science* **257**, 665–669.
10. Yuste, R., Nelson, D. A., Rubin, W. W. & Katz, L. C. (1995) *Neuron* **14**, 7–17.
11. Kandler, K. & Katz, L. C. (1998) *J. Neurosci.* **18**, 1419–1427.
12. Yuste, R. & Katz, L. C. (1991) *Neuron* **6**, 333–344.
13. Owens, D. F., Boyce, L. H., Davis, M. B. & Kriegstein, A. R. (1996) *J. Neurosci.* **16**, 6414–6423.
14. Aniksztejn, L., Sciancalepore, M., Ben Ari, Y. & Cherubini, E. (1995) *J. Neurophysiol.* **73**, 1422–1429.
15. Woodhall, G., Gee, C. E., Robitaille, R. & Lacaille, J. C. (1999) *J. Neurophysiol.* **81**, 371–382.
16. Pasti, L., Volterra, A., Pozzan, T. & Carmignoto, G. (1997) *J. Neurosci.* **17**, 7817–7830.
17. Berridge, M. J., Bootman, M. D. & Lipp, P. (1998) *Nature (London)* **395**, 645–648.
18. Berridge, M. J. (1997) *Nature (London)* **386**, 759–760.
19. De Koninck, P. & Schulman, H. (1998) *Science* **279**, 227–230.
20. Dupont, G. & Goldbeter, A. (1998) *BioEssays* **20**, 607–610.
21. Li, W., Llopis, J., Whitney, M., Zlokarnik, G. & Tsien, R. Y. (1998) *Nature (London)* **392**, 936–941.
22. Dolmetsch, R. E., Xu, K. & Lewis, R. S. (1998) *Nature (London)* **392**, 933–936.
23. Gu, X. & Spitzer, N. C. (1995) *Nature (London)* **375**, 784–787.
24. Kawabata, S., Tsutsumi, R., Kohara, A., Yamaguchi, T., Nakanishi, S. & Okada, M. (1996) *Nature (London)* **383**, 89–92.
25. Nakahara, K., Okada, M. & Nakanishi, S. (1997) *J. Neurochem.* **69**, 1467–1475.
26. Flint, A. C., Liu, X. & Kriegstein, A. R. (1998) *Neuron* **20**, 43–53.
27. LoTurco, J. J., Owens, D. F., Heath, M. J. S., Davis, M. B. E. & Kriegstein, A. R. (1995) *Neuron* **15**, 1287–1298.
28. Blanton, M. G., LoTurco, J. J. & Kriegstein, A. R. (1989) *J. Neurosci. Methods* **30**, 203–210.
29. Romano, C., van den Pol, A. N. & O'Malley, K. L. (1996) *J. Comp. Neurol.* **367**, 403–412.
30. Linden, D. J., Smeyne, M. & Connor, J. A. (1994) *J. Neurophysiol.* **71**, 1992–1998.
31. Cornell-Bell, A. H., Finkbeiner, S. M., Cooper, M. S. & Smith, S. J. (1990) *Science* **247**, 470–473.
32. Charles, A. C., Merrill, J. E., Dirksen, E. R. & Sanderson, M. J. (1991) *Neuron* **6**, 983–992.
33. Dani, J. W., Chernjavsky, A. & Smith, S. J. (1992) *Neuron* **8**, 429–440.
34. Holzwarth, J. A., Gibbons, S. J., Brorson, J. R., Philipson, L. H. & Miller, R. J. (1994) *J. Neurosci.* **14**, 1879–1891.
35. Schwartz, T. H., Rabinowitz, D., Unni, V., Kumar, V. S., Smetters, D. K., Tsiola, A. & Yuste, R. (1998) *Neuron* **20**, 541–552.
36. Hajnoczky, G., Robb-Gaspers, L. D., Seitz, M. B. & Thomas, A. P. (1995) *Cell* **82**, 415–424.
37. Lledo, P. M., Hjelmstad, G. O., Mukherji, S., Soderling, T. R., Malenka, R. C. & Nicoll, R. A. (1995) *Proc. Natl. Acad. Sci. USA* **92**, 11175–11179.
38. Stevens, C. F., Tonegawa, S. & Wang, Y. (1994) *Curr. Biol.* **4**, 687–693.
39. Silva, A. J., Paylor, R., Wehner, J. M. & Tonegawa, S. (1992) *Science* **257**, 206–211.
40. Blue, M. E. & Parnavelas, J. G. (1983) *J. Neurocytol.* **12**, 697–712.
41. Juraska, J. M. & Fifkova, E. (1979) *J. Comp. Neurol.* **183**, 257–267.
42. Crair, M. C. & Malenka, R. C. (1995) *Nature (London)* **375**, 325–328.
43. Dolmetsch, R. E., Lewis, R. S., Goodnow, C. C. & Healy, J. I. (1997) *Nature (London)* **386**, 855–858.
44. Finkbeiner, S. & Greenberg, M. E. (1998) *J. Neurobiol.* **37**, 171–189.
45. Ferrari, M. B., Rohrbough, J. & Spitzer, N. C. (1996) *Dev. Biol.* **178**, 484–497.
46. Spitzer, N. C. (1995) *Perspect. Dev. Neurobiol.* **2**, 379–386.